Published in final edited form as:
Curr Biol. 2008 May 20; 18(10): 745–750.

Spatial regulation of *nanos* is required for its function in dendrite morphogenesis

Jillian L. Brechbiel and **Elizabeth R. Gavis***
Department of Molecular Biology, Princeton University, Princeton, NJ 08544

Summary

Spatial control of mRNA translation is a well established mechanism for generating cellular asymmetries and for functional specialization of polarized cells like neurons. A requirement for the translational repressor Nanos (Nos) in the *Drosophila* larval peripheral nervous system (PNS) implicates translational control in dendrite morphogenesis [1]. Nos was first identified by its requirement in the posterior of the early embryo for abdomen formation [2]. Nos synthesis is targeted to the posterior pole of the oocyte and early embryo through translational repression of unlocalized *nos* mRNA coupled with translational activation of *nos* mRNA localized at the posterior pole [3,4]. Mutations that abolish *nos* localization prevent abdominal development whereas de-repression of unlocalized *nos* mRNA suppresses head/thorax development, indicating that spatial regulation of *nos* is essential for anterior-posterior patterning [3,5]. The observation that both loss and overexpression of Nos affect dendrite branching complexity in class IV dendritic arborization (da) neurons suggests that *nos* might also be regulated in these larval sensory neurons [1]. Here we show that localization and translational control of *nos* mRNA are essential for late stages of da neuron morphogenesis. RNA-protein interactions that regulate *nos* translation in the oocyte and early embryo also regulate *nos* in the PNS. Live imaging of *nos* mRNA shows that the cis-acting signal responsible for posterior localization in the oocyte/embryo mediates localization to the processes of class IV da neurons, but suggests a different transport mechanism. The need to target *nos* mRNA to the processes of da neurons may reflect a requirement for Nos protein in controlling translation locally within dendrites.

Results and Discussion

Nos is Required in Da Neurons to Maintain Dendrite Complexity

Da neurons, which innervate the larval epidermis, can be divided into four classes based on the complexity of their dendritic arbors, with class IV being the most highly branched [6]. These neurons elaborate primary and secondary branches during the first instar stage of larval development. By the second instar stage, higher order branches extend to completely cover the larval body wall [7]. Complete, nonredundant coverage or “tiling” of the epidermis by class IV da neurons is maintained throughout larval development [8]. Mutation of *nos* results in a reduction in the number of higher order branches of class IV da neurons without affecting the morphology of the main branches [1]. This decreased branching complexity could reflect an early role for *nos* in the initial elaboration of the dendritic branches or a later role in maintaining coverage of the receptive field during larval growth. To distinguish between these possibilities,

*Author for correspondence: lgavis@princeton.edu, Phone: (609) 258-3857, FAX: (609) 258-1343.

we examined the morphology of *nos* mutant class IV da neurons at different larval stages. In these, and all subsequent experiments, class IV da neurons are marked by mCD8:GFP, expressed using the $GAL4^{477}$ driver [9]. Branching complexity was monitored by quantitation of branch termini (see Supplemental Experimental Procedures and Figure 1 legend).

From the first larval instar through the early third instar stage, da neurons in wild-type larvae, *nos* mutant larvae, and *nos* mutant larvae carrying a genomic *nos* transgene, *gnos* [3], show no significant difference in branching complexity (Figure 1A–C, G and data not shown). Morphological defects are first detected at the late third instar stage, when a significant reduction of higher order branching is observed in *nos* mutant da neurons as compared to wild-type neurons (Figure 1D,E). Whereas terminal branch density decreases slightly as body size increases from early to late third instar stages in wild-type larvae, the density of terminal branches decreases dramatically in *nos* mutant larvae (Fig. 1G). Wild-type branching is restored in *nos* mutant larvae by addition of *gnos*, which includes native transcriptional regulatory sequences required for *nos* expression and rescues all *nos* mutant embryonic phenotypes [3,10] (Figure 1F,G). These results indicate that Nos is not required for the initial elaboration of dendritic branches but instead plays a role at later stages of development, possibly by maintaining existing branches or promoting new branch extension during larval growth.

nos is Localized to the Processes of Da Neurons

Localized translation of *nos* required for embryonic patterning is achieved through a combination of mRNA localization and translational control. To determine if *nos* is spatially regulated in da neurons, we analyzed the distribution of *nos* mRNA by modifying a fluorescent labeling method previously used to investigate the mechanism of *nos* mRNA localization during oogenesis [4]. In this method, a fusion between bacteriophage MS2 coat protein (MCP) and either GFP or RFP is tethered to *nos* mRNA bearing 6 stem-loop binding sites for MCP [$nos\text{-}(ms2)_6$]. Here, we have improved detection of *nos* by introducing 18 MCP-binding stem-loops [$nos\text{-}(ms2)_{18}$]. The $nos\text{-}(ms2)_{18}$ transgene behaves indistinguishably from *gnos* and the previously described $nos\text{-}(ms2)_6$ transgenes in the oocyte and early embryo (K. Forrest and E.R.G., unpublished). To label $nos\text{-}(ms2)_{18}$ RNA specifically in da neurons, we expressed MCP-RFP under UAS control using $GAL4^{477}$ in larvae carrying the $nos\text{-}(ms2)_{18}$ transgene. In neurons from control larvae that express MCP-RFP without $nos\text{-}(ms2)_{18}$ mRNA, RFP fluorescence is largely confined to the nucleus due to a nuclear localization signal engineered in MCP-RFP that targets unbound MCP-RFP to the nucleus (Fig. 2A). By contrast, RFP-labeled $nos\text{-}(ms2)_{18}$ mRNA (*nos*RFP*) can be detected in the cell body and in particles that are distributed along the dendrites and axons of class IV da neurons (Fig. 2B). Analysis of *nos*RFP* throughout larval development showed that localization of *nos* to the processes of da neurons can first be detected early at the third instar stage (data not shown).

We have not been able to confirm localization of native *nos* mRNA in da neurons by in situ hybridization methods, most likely due to a combination of low transcript abundance and high background from the underlying muscle tissue. However, we have previously shown that fluorescently labeled *nos* mRNA is a valid proxy for native *nos* mRNA in the oocyte and embryo [4]. Moreover, the correlation between dendritic localization of *nos*RFP* and its ability to rescue the *nos* mutant dendritic branching defect, described below, gives us confidence that it recapitulates the distribution of native *nos* in these neurons.

The *nos* 3′UTR is Required for Efficient *nos* Localization in the PNS

Posterior localization of *nos* in the oocyte and early embryo is mediated by a complex cis-acting localization signal in the *nos* 3′ untranslated region (3′UTR) comprising multiple, partially functional localization elements [11]. To test whether the same sequences direct

dendritic localization of *nos* in da neurons, we analyzed the distribution of RFP-labeled *nos–(ms2)$_{18}$* RNAs bearing 3′UTR deletions (Figure S1A). Deletion of the entire localization signal (*nos*Δ*LS*) or three of the four localization elements (*nos+1*), respectively, abolishes or severely reduces posterior localization of *nos* in the oocyte and embryo [11]. Both deletions also compromise localization to the processes of da neurons (Figure 2C and data not shown). Quantitation of *nos*RFP* particles shows reduced accumulation in dendrites of larvae expressing *nos+1-(ms2)$_{18}$* mRNA relative to larvae expressing *nos-(ms2)$_{18}$* mRNA, whereas no significant difference is detected within the cell body (Figure 2E). In contrast, the distribution of RFP-labeled *nos+2-(ms2)$_{18}$* mRNA is similar to that of *nos-(ms2)$_{18}$*mRNA (Figure 2D,E). This RNA lacks two of the four localization elements but retains the *nos* +2 element, which confers near wild-type localization in the embryo [11]. The *nos+1-(ms2)$_{18}$* and *nos+2-(ms2)$_{18}$* transcripts are present at comparable levels in da neurons as determined by RT-PCR (Figure S2) and similar results were obtained for two independent lines of each transgene (data not shown), indicating that the observed difference in localization to neuronal processes is not likely due to a difference in expression or stability. Thus, the same sequences that mediate posterior localization of *nos* at earlier developmental stages target *nos* to the processes of class IV da neurons. This result suggests that one or more factors that recognize this localization signal to mediate localization during oogenesis may be used again for dendritic localization.

Localization of *nos* is Required for its Function in the PNS

Since posterior localization of *nos* is essential for its function in embryonic development, we investigated whether dendritic localization of *nos* is also required for its function in the larval PNS. The *nos-(ms2)$_{18}$*, *nos+1-(ms2)$_{18}$* and *nos+2-(ms2)$_{18}$* transgenes were introduced into *nos* mutant larvae and assayed for their ability to rescue the *nos* mutant dendritic defect. All three transgenes include sequences required for *nos* translational regulation (see below) and none of these transgenes on its own affects dendrite branching complexity (data not shown). Class IV da neurons in *nos* mutant larvae carrying either the *nos-(ms2)$_{18}$* or *nos+2-(ms2)$_{18}$* transgene exhibit nearly wild-type dendritic branching, indicating that both transgenes are able to rescue the *nos* mutant phenotype (Figure 3A–C, E). In contrast, the *nos+1-(ms2)$_{18}$* transgene fails to rescue, as larvae show reduced branching complexity (Figure 3D,E).

These results indicate that the localization of *nos* to class IV da neurons is required for *nos* function in dendrite morphogenesis. Because currently available anti-Nos antibodies are not adequate to detect Nos protein in da neurons (our data, also see Ref. [1]), we cannot show definitively that *nos* mRNA localization leads to local production of Nos protein. However, the correlation between the localization to neuronal processes and the ability to rescue the *nos* mutant branching defect revealed by the *nos+1-(ms2)$_{18}$* and *nos+2-(ms2)$_{18}$* mRNAs provides strong evidence that *nos* mRNA localization plays a critical role by targeting synthesis of Nos to dendrites.

Live imaging of *nos* mRNA Particle Movement in Da Neurons

Although most mRNAs are thought to be transported as particles along cytoskeletal elements by motor proteins, *nos* accumulates at the posterior of the oocyte by a passive diffusion and entrapment mechanism [4]. As a first step toward investigating the mechanism of *nos* localization in da neurons, we performed time lapse imaging of *nos*RFP* in da neurons of intact larvae at high magnification and time resolution. Control neurons expressing only MCP-RFP contain few RFP-labeled particles outside of the cell body and these particles rarely exhibit movement (Movie S1). In contrast, in neurons expressing *nos*RFP*, dynamic particles are readily detected in the cell body and processes (Figure 2F–H and Movie S2). Photobleaching of RFP that occurs at the requisite high image capture rates and the potential for tissue damage limits our time sequences to ≤90 sec. During these short periods, we observe particles traveling with linear trajectories, in both anterograde and retrograde directions along the neuronal

processes, and in some cases, individual particles exhibit bi-directional movement (Figure 2F–H;Movie S2). By analyzing sustained particle runs in a single direction (average run distance = 4.1 μm; see Supplemental Experimental Procedures) within the dendrites of five neurons from three independent larvae, we calculated a mean average dendritic particle velocity of 0.56 μm/sec (range=0.21–0.97 μm/sec, n=40). This value is similar to those we have observed, using the same labeling method, for dynein-dependent transport of *bicoid* (*bcd*) mRNA in the Drosophila oocyte [12] and similar rates have been observed for microtubule-dependent transport of ribonucleoprotein particles in the dendrites of cultured hippocampal neurons [13–16]. Like *nos*, these dendritic RNA-containing particles exhibit bi-directional movement. The generation of brighter and more photostable MCP fusion proteins that permit visualization of particles over longer time periods and in various mutant backgrounds will enable us to determine how these complex particle dynamics lead to accumulation of RNA in dendrites.

Whereas localization of *nos* during oogenesis occurs by diffusion and entrapment [4], the trajectories and velocities exhibited by dendritic *nos* particles are characteristic of cytoskeletal-based transport. Analysis of microtubule polarity in da neurons indicates that the majority of microtubules are oriented with their minus ends distal to the cell body [17]. Although individual da neuron subclasses were not distinguished in this study, the observations suggest that transport of *nos* mRNA particles into dendrites utilizes dynein. *nos* RNA injected into blastoderm embryos exhibits microtubule-dependent apical localization characteristic of pair-rule transcripts, whose transport is dynein-mediated [18,19]. Since endogenous *nos* mRNA is not apically localized, the significance of such transport has been unclear. Our results suggest that the ability of *nos* to engage dynein-dependent transport machinery is indeed relevant to its role in the PNS.

Regulation of Dendrite Morphogenesis by Glo and Smg

Translational activation of *nos* at the posterior pole is tightly coupled to translational repression of unlocalized *nos* mRNA to prevent accumulation of Nos in the anterior of the embryo, where Nos suppresses anterior development [5]. Since *nos* localization during oogenesis is inefficient, this linkage is essential to silence *nos* mRNA that remains distributed throughout the bulk cytoplasm [20]. Translational repression of *nos* mRNA is mediated by a structural motif, the translational control element (TCE), within the *nos* 3′UTR [21–23] (Figure S1B). TCE function requires the formation of two stem-loops, designated as II and III, that have temporally distinct activities [24,25]. Whereas stem-loop III mediates repression of *nos* during oogenesis, through its interaction with Glorund (Glo), stem-loop II is responsible for repression of *nos* in the early embryo, through its interaction with a different repressor, Smaug (Smg) [26–28].

Replacement of the *nos* 3′UTR by *α-tubulin* 3′UTR sequences (*nos-tub3′UTR*) abolishes *nos* localization and translational repression, leading to unrestricted synthesis of Nos and defects in anterior development [5]. GAL4 mediated overexpression of a *UAS-nos-tub3′UTR* transgene in class IV da neurons is also deleterious, causing decreased branching complexity. This overexpression phenotype is ameliorated by reinsertion of the *nos* TCE [1]. The observation that both loss and overexpression of *nos* cause similar defects indicates that although *nos* is required for dendrite morphogenesis, the level of Nos protein must be carefully modulated in da neurons. Moreover, the ability of the TCE to suppress the toxicity of *nos* mRNA overexpression in da neurons suggests that it may normally function to control Nos levels in the PNS. We therefore sought to determine whether endogenous *nos* is regulated by the TCE in da neurons.

Ectopic expression studies have identified several additional somatic cell types where the TCE can repress translation, including neuroendocrine cells and the dorsal pouch epithelium [29, 30]. However, TCE function in the dorsal pouch does not depend on the Glo or Smg binding sites, but requires a distinct sequence motif with homology to the Bearded (Brd) box [29].

Mutation of the Brd box-like motif does not abrogate the ability of the TCE to suppress excess *nos* activity in da neurons (data not shown). Consequently, to determine whether endogenous *nos* mRNA might be regulated by the TCE, we first analyzed da neurons in *glo* and *smg* mutant larvae.

Larvae mutant for *glo* or *smg* survive until third instar stage, permitting us to examine the effect of eliminating either repressor on dendrite morphology of da neurons. Compared to wild-type class IV da neurons, *glo* mutant larvae show a significant decrease in the number of higher order dendritic branches as reflected by a decreased number of terminal dendritic processes (Figure 4G). Because *glo* mutant larvae exhibit additional defects (J.L.B. and E.R.G., unpublished), we disrupted *glo* function specifically in class IV da neurons either by using $GAL4^{477}$ to express a *UAS-gloRNAi* transgene or by using the MARCM method [31] to generate mosaic animals. In both cases, *glo* mutant da neurons show decreased branching complexity (Figure 4A–C,G). Mutation of *smg* or $GAL4^{477}$-mediated overexpression of a *UAS-smg* transgene also causes loss of high order branches (Figure 4D,E,G). Larvae doubly mutant for *glo* and *smg* do not show a more severe phenotype than larvae mutant for either gene alone (Figure 4F,G), suggesting that each repressor contributes independently. Thus, defects due to loss or overexpression of the repressors are consistent with defects caused by loss or overexpression of *nos*. Due to the aforementioned inadequacy of anti-Nos antibodies, we have not been able to monitor changes in Nos protein levels in *glo* and *smg* mutant da neurons. However, when combined with the analysis of Glo and Smg binding site mutations presented below, these results strongly support a role for *glo* and *smg* in regulation of *nos* for dendrite morphogenesis.

TCE-dependent Translational Regulation of *nos* is Required for Dendrite Development

In the oocyte, Glo binds specifically to the distal double-stranded helix of TCE stem-loop III (the Glo Recognition Helix or GRH; Figure S1B) [27]. In the embryo, Smg interacts with *nos* TCE stem-loop II, via nucleotides within the loop designated as the Smg Recognition Element (SRE; Figure S1B) [22, 24]. A second SRE located downstream of the TCE in the *nos* 3′UTR appears to act redundantly [22, 23]. To determine whether the defects observed in *glo* and *smg* mutant da neurons are due to loss of TCE-mediated repression, we tested whether mutation of the *nos* GRH or SREs produces a similar phenotype. Mutations that disrupt both SREs ($SREs^{-}$), the binding site for Glo (GRH^{-}), or the SREs and GRH ($SREs^{-}GRH^{-}$) together (Figure S1B) were introduced into the *gnos* transgene. The resulting $gnosSREs^{-}$, $gnosGRH^{-}$, a*nd* $gnosSREs^{-}GRH^{-}$ transgenes all produce mRNAs that show wild-type localization in the early embryo but whose translation is not restricted to the posterior pole (Ref [10]; E.R.G., unpublished). When compared to larvae expressing the wild-type *gnos* transgene, branching complexity is significantly reduced in da neurons of larvae expressing $gnosSREs^{-}$, $gnosGRH^{-}$, a*nd* $gnosSREs^{-}GRH^{-}$ transgenes (Figure 5). Moreover, each of these transgenes behaves similarly to the *gnos-tub3′UTR* transgene, which lacks the entire *nos* 3′UTR, indicating that mutation of the GRH and/or SREs is sufficient to disrupt *nos* regulation in the PNS. Together, these results show that TCE-mediated regulation of *nos* in da neurons is essential for dendrite morphogenesis. Furthermore, the finding that the same phenotype is produced by either eliminating the repressors or mutating their binding sites provides strong evidence that this regulation is mediated by Glo and Smg.

In many cell types, protein synthesis is spatially regulated through the transport of translationally silent mRNAs and activation of these mRNAs at the target destination. Linkage of translation and localization serves not only to prevent premature accumulation of *nos* during transit to the oocyte posterior, but to silence the large pool of *nos* that remains unlocalized due to inefficient posterior localization [20]. We cannot yet distinguish whether localization of *nos* in da neurons is similarly inefficient or whether translational repression of *nos* serves

primarily to repress translation during transport. However, the deleterious effect on dendrite morphogenesis caused by mutations that disrupt TCE function show that, as for maternally synthesized *nos* mRNA, localization alone is not sufficient to modulate its activity.

Conclusions

nos plays an important role in dendrite morphogenesis and we show that *nos* function in da neurons requires spatial regulation of *nos* mRNA. Cis-acting sequences and two cognate factors that control *nos* mRNA localization and/or translation in the oocyte and early embryo are redeployed during larval stages to regulate localization and translation of *nos* in da neurons. Localization of *nos* mRNA to the processes of class IV da neurons is essential for dendritic branching. For the first time, we observe movement of RNA particles in neurons of intact animals and analysis of *nos* mRNA particle movement suggests that *nos* localization occurs by different mechanisms depending on cellular context. Taken together, our results support a role for Nos as a local regulator of translation in the PNS.

In the early embryo, Nos functions in a complex with the RNA-binding protein Pumilio (Pum) to repress *hunchback* mRNA translation, thereby promoting abdominal development [32,33]. Whereas Pum is produced throughout the embryo [33,34], restriction of Nos synthesis to the posterior limits the spatial domain of the repressor complex. Mutations in *nos* and *pum* produce similar defects in dendrite morphogenesis, suggesting that Nos and Pum also act together to repress translation in da neurons [1]. Thus, spatial regulation of *nos* may serve a similar function in the PNS as it does in the early embryo, by restricting the activity of the Nos/Pum repressor complex to dendrites.

Supplementary Material

Refer to Web version on PubMed Central for supplementary material.

Acknowledgements

We are grateful to K. Forrest for initiating this project by generating and characterizing the *nos-(ms2)$_{18}$* and *UAS-MCP-RFP* transgenic lines, T. Weil for assistance with particle movement analysis and preparation of the Supplemental Movies, A. Becalska for generation of *nos+2-(ms2)$_{18}$* transgenic lines, and N. Jeurkar for generation of *UASp-smg* transgenic lines. We also thank Y.N. Jan and R. Wharton for fly stocks, B. Ye, U. Mayor, and W. Grueber for technical advice, J. Goodhouse (Princeton) and A. Sossick (Gurdon Institute) for microscopy assistance, and B. Ye, T. Weil, and I. Clark for comments on the manuscript. E.R.G. thanks her sabbatical host A. Brand and members of the Brand lab for hospitality during this work. This work was supported initially by the NSF (IOB-0344728) and subsequently by the NIH (R01 GM061107, R01 GM067758).

References

1. Ye B, Petritsch C, Clark IE, Gavis ER, Jan LY, Jan YN. *nanos* and *pumilio* are essential for dendrite morphogenesis in *Drosophila* peripheral neurons. Curr Biol 2004;14:314–321. [PubMed: 14972682]
2. Lehmann R, Nusslein-Volhard C. The maternal gene *nanos* has a central role in posterior pattern formation of the *Drosophila* embryo. Development 1991;112:679–691. [PubMed: 1935684]
3. Gavis ER, Lehmann R. Localization of *nano*s RNA controls embryonic polarity. Cell 1992;71:301–313. [PubMed: 1423595]
4. Forrest KM, Gavis ER. Live imaging of endogenous mRNA reveals a diffusion and entrapment mechanism for *nanos* mRNA localization in *Drosophila*. Curr Biol 2003;13:1159–1168. [PubMed: 12867026]
5. Gavis ER, Lehmann R. Translational regulation of *nanos* by RNA localization. Nature 1994;369:315–318. [PubMed: 7514276]
6. Grueber WB, Jan LY, Jan YN. Tiling of the *Drosophila* epidermis by multidendritic sensory neurons. Development 2002;129:2867–2878. [PubMed: 12050135]

7. Gao FB, Brenman JE, Jan LY, Jan YN. Genes regulating dendritic outgrowth, branching, and routing in *Drosophila*. Genes Dev 1999;13:2549–2561. [PubMed: 10521399]
8. Grueber WB, Ye B, Moore AW, Jan LY, Jan YN. Dendrites of distinct classes of *Drosophila* sensory neurons show different capacities for homotypic repulsion. Curr Biol 2003;13:618–626. [PubMed: 12699617]
9. Grueber WB, Jan LY, Jan YN. Different levels of the homeodomain protein Cut regulate distinct dendrite branching patterns of *Drosophila* multidendritic neurons. Cell 2003;112:805–818. [PubMed: 12654247]
10. Gavis ER, Chatterjee S, Ford NR, Wolff LJ. Dispensability of *nanos* mRNA localization for abdominal patterning but not for germ cell development. Mech Dev 2008;125:81–90. [PubMed: 18036786]
11. Gavis ER, Curtis D, Lehmann R. Identification of cis-acting sequences that control *nanos* RNA localization. Dev Biol 1996;176:36–50. [PubMed: 8654893]
12. Weil TT, Forrest KM, Gavis ER. Localization of *bicoid* mRNA in late oocytes is maintained by continual active transport. Dev. Cell 2006;11:251–262.
13. Rook MS, Lu M, Kosik KS. CaMKIIalpha 3′ untranslated region-directed mRNA translocation in living neurons: visualization by GFP linkage. J Neurosci 2000;20:6385–6393. [PubMed: 10964944]
14. Knowles RB, Sabry JH, Martone ME, Deerinck TJ, Ellisman MH, Bassell GJ, Kosik KS. Translocation of RNA granules in living neurons. J Neurosci 1996;16:7812–7820. [PubMed: 8987809]
15. Kohrmann M, Luo M, Kaether C, DesGroseillers L, Dotti CG, Kiebler MA. Microtubule-dependent recruitment of Staufen-green fluorescent protein into large RNA-containing granules and subsequent dendritic transport in living hippocampal neurons. Mol Biol Cell 1999;10:2945–2953. [PubMed: 10473638]
16. Kanai Y, Dohmae N, Hirokawa N. Kinesin transports RNA: isolation and characterization of an RNA-transporting granule. Neuron 2004;43:513–525. [PubMed: 15312650]
17. Rolls MM, Satoh D, Clyne PJ, Henner AL, Uemura T, Doe CQ. Polarity and intracellular compartmentalization of *Drosophila* neurons. Neural Develop 2007;2:7. [PubMed: 17470283]
18. Bullock SL, Ish-Horowicz D. Conserved signals and machinery for RNA transport in *Drosophila* oogenesis and embryogenesis. Nature 2001;414:611–616. [PubMed: 11740552]
19. Wilkie GS, Davis I. Drosophila *wingless* and pair-rule transcripts localize apically by dynein-mediated transport of RNA particles. Cell 2001;105:209–219. [PubMed: 11336671]
20. Bergsten SE, Gavis ER. Role for mRNA localization in translational activation but not spatial restriction of *nanos* RNA. Development 1999;126:659–669. [PubMed: 9895314]
21. Gavis ER, Lunsford L, Bergsten SE, Lehmann R. A conserved 90 nucleotide element mediates translational repression of *nanos* RNA. Development 1996;122:2791–2800. [PubMed: 8787753]
22. Smibert CA, Wilson JE, Kerr K, Macdonald PM. Smaug protein represses translation of unlocalized *nanos* mRNA in the *Drosophila* embryo. Genes Dev 1996;10:2600–2609. [PubMed: 8895661]
23. Dahanukar A, Wharton RP. The Nanos gradient in *Drosophila* embryos is generated by translational regulation. Genes Dev 1996;10:2610–2620. [PubMed: 8895662]
24. Crucs S, Chatterjee S, Gavis ER. Overlapping but distinct RNA elements control repression and activation of *nanos* translation. Mol. Cell 2000;5:457–467.
25. Forrest KM, Clark IE, Jain RA, Gavis ER. Temporal complexity within a translational control element in the *nanos* mRNA. Development 2004;131:5849–5857. [PubMed: 15525666]
26. Smibert CA, Lie YS, Shillingaw W, Henzel WJ, Macdonald PM. Smaug, a novel and conserved protein contributes to repression of *nanos* mRNA translation in vitro. RNA 1999;5:1535–1547. [PubMed: 10606265]
27. Kalifa Y, Huang T, Rosen LN, Chatterjee S, Gavis ER. Glorund, an hnRNP F/H homolog, is an ovarian repressor of *nanos* translation. Dev. Cell 2006;10:291–301.
28. Dahanukar A, Walker JA, Wharton RP. Smaug, a novel RNA-binding protein that operates a translational switch in *Drosophila*. Mol. Cell 1999;4:209–218.

29. Duchow HK, Brechbiel JL, Chatterjee S, Gavis ER. The *nanos* translational control element represses translation in somatic cells by a Bearded box-like motif. Dev Biol 2005;282:207–217. [PubMed: 15936341]

30. Clark IE, Duchow HK, Vlasak AN, Gavis ER. A common translational control mechanism functions in axial patterning and neuroendocrine signaling in *Drosophila*. Development 2002;129:3325–3334. [PubMed: 12091303]

31. Lee T, Luo L. Mosaic analysis with a repressible cell marker for studies of gene function in neuronal morphogenesis. Neuron 1999;22:451–461. [PubMed: 10197526]

32. Sonoda J, Wharton RP. Recruitment of Nanos to *hunchback* mRNA by Pumilio. Genes Dev 1999;13:2704–2712. [PubMed: 10541556]

33. Barker DD, Wang C, Moore J, Dickinson LK, Lehmann R. Pumilio is essential for function but not for distribution of the *Drosophila* abdominal determinant Nanos. Genes Dev 1992;6:2312–2326. [PubMed: 1459455]

34. Macdonald PM. The Drosophila *pumilio* gene: an unusually long transcription unit and an unusual protein. Development 1992;114:221–232. [PubMed: 1576962]

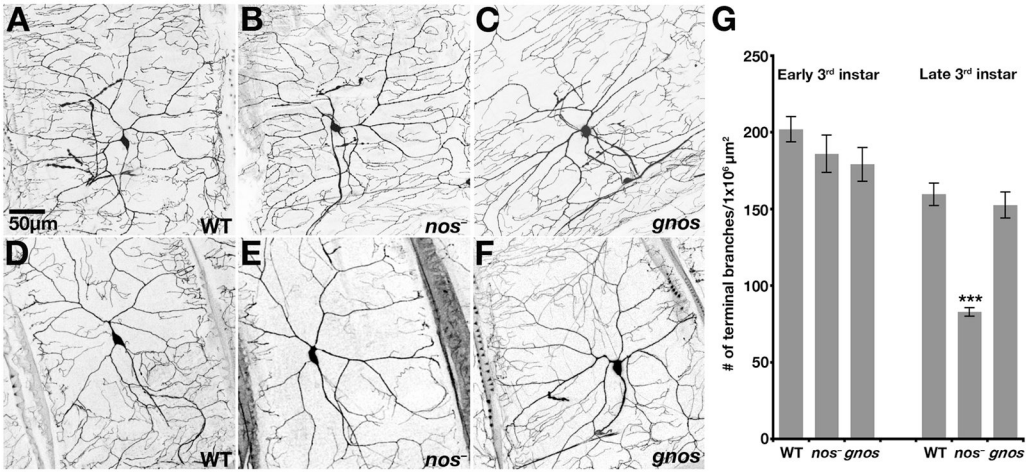

Figure 1. *nos* Plays a Role in Maintenance of Dendritic Branching

Confocal Z-series projections of class IV da neurons in (A–C) early third instar larvae and (D–F) late third instar larvae. Da neurons are marked here and in all subsequent figures by using *GAL4*^{477} to drive expression of *UAS-mcd8:GFP*. (A,D) Neurons from wild-type larvae. (B,E) Neurons from *nos* mutant larvae. (C,F) Neurons from *nos* mutant larvae carrying the *gnos* rescue transgene. (G) Quantitation of total number of terminal branches within a 1×10^6 μm^2 region of the dendritic tree of an individual neuron (see Experimental Procedures). Values are the average +/− standard error. One neuron per larva was analyzed from early third instar: wild-type (n=10 neurons); *nos* mutant (n=9 neurons); *gnos* (n=10 neurons); or late third instar: wild-type (n=15 neurons); *nos* mutant (n=10 neurons); *gnos* (n=10 neurons). Here and in all subsequent figures, P values were determined by the Student's t-test and are labeled as *, **, and *** to denote $p<0.05$, $p<0.01$ and $p<0.001$ respectively.

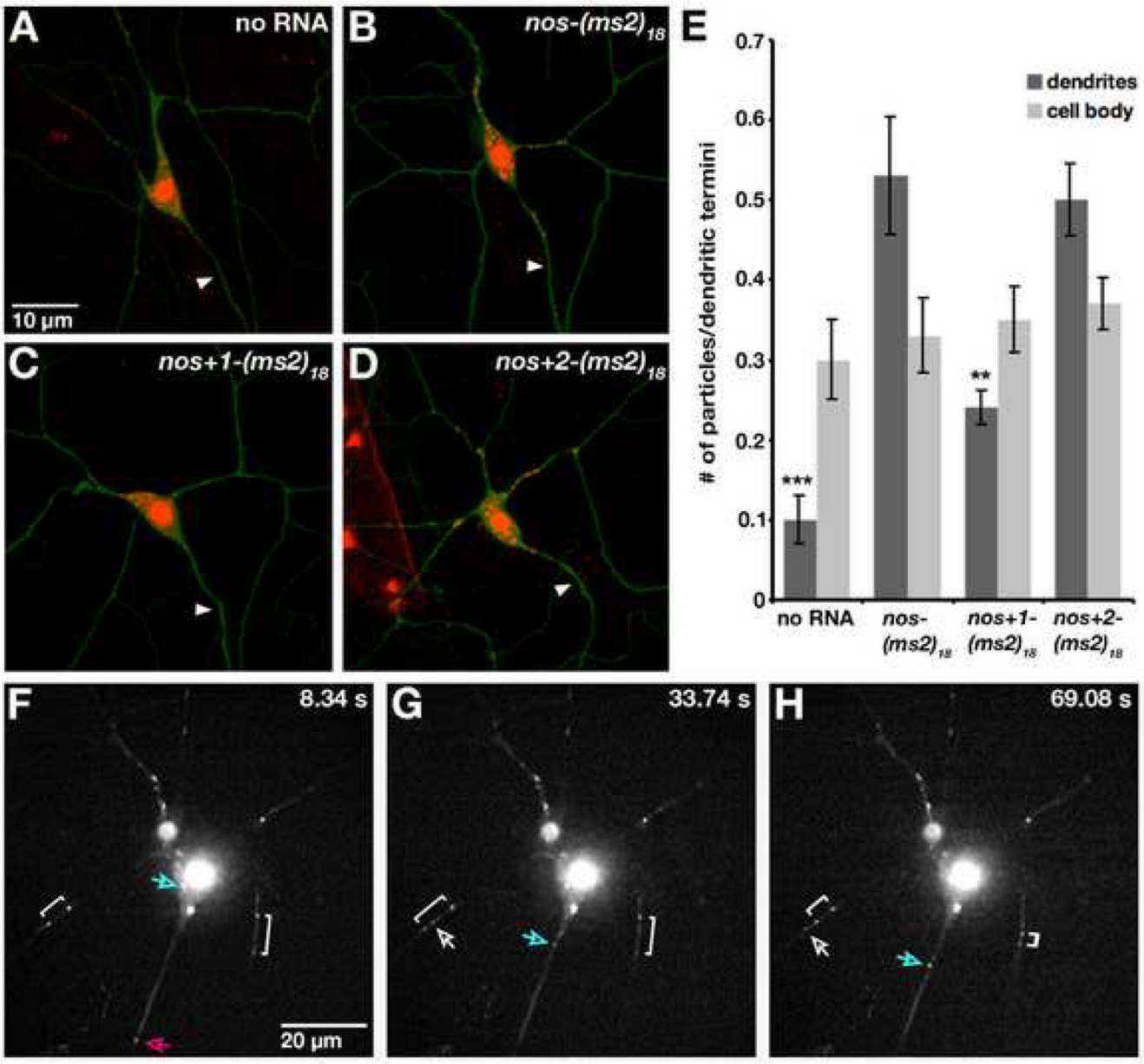

Figure 2. Localization of *nos* to the Processes of Da Neurons

(A–D) Class IV da neurons in semi-intact third instar larvae expressing mCD8:GFP, MCP-RFP and (A) no ms2-tagged *nos* mRNA (control); (B) *nos-(ms2)$_{18}$* mRNA; *(C) nos+1-(ms2)$_{18}$* mRNA; (D) *nos+2-(ms2)$_{18}$* mRNA. MCP-RFP that is not bound to mRNA is sequestered in the nucleus due to an NLS in the MCP-RFP fusion protein. Arrowhead indicates the axon, as identified in lower power images. (E) Quantitation of *nos*RFP* particles in dendritic branches. All neurons were imaged using identical confocal settings. A merged image showing both green (mcd8:GFP) and red (*nos*RFP* or MCP-RFP alone) channels was enlarged and adjusted in Adobe Photoshop so that green channel was just visible. Red particles encompassed within the branches or cell body were counted and each total was normalized to the total number of dendritic termini within the field imaged (3.6×10^4 μm^2). Two independent lines analyzed for each transgene produced similar results and one line for each is shown. For each genotype, values are the average +/− standard error for 10 neurons. (F–H) Time lapse

sequence of RFP-labeled *nos-(ms2)$_{18}$* mRNA in a Class IV da neuron (only the red channel is shown). Each panel shows a single confocal section captured at the indicated time. See Supplemental Movie S2 for the complete 75 second time series. Examples of movement are indicated. Brackets illustrate movement toward and away from the cell body. Particles indicated by the bracket on the left move bidirectionally – first apart from each other, then toward each other. The pink arrow illustrates a particle that moves out of the frame. The white arrow shows a particle that crosses paths with one of the particles indicated by the bracket. The blue arrow marks a particle traveling from the cell body to a dendrite.

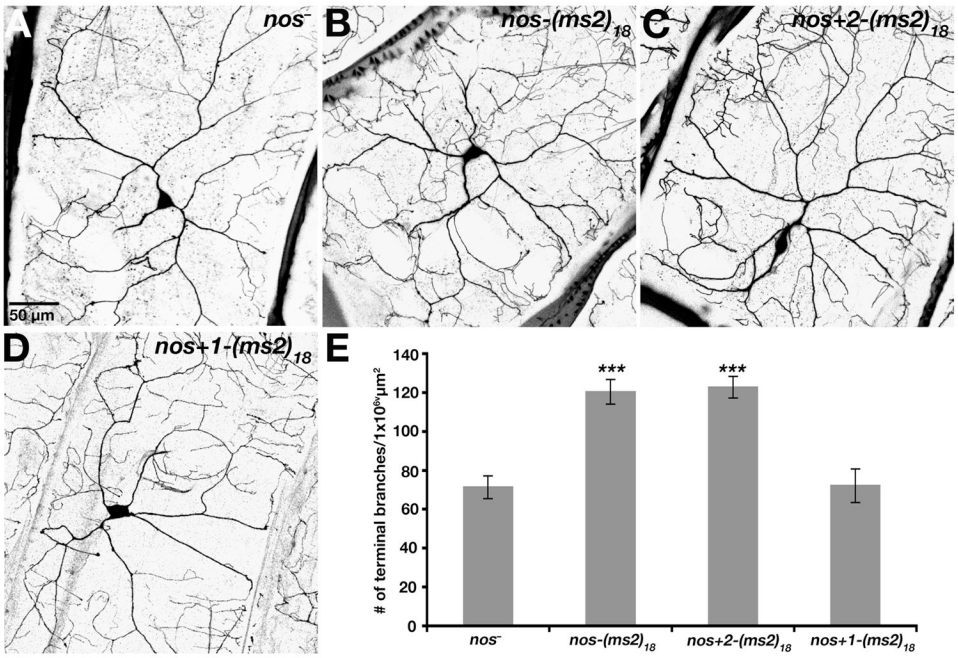

Figure 3. *nos* mRNA Localization is Required for Dendrite Morphogenesis

The *nos* transgenes analyzed in Fig. 2 were tested for their ability to rescue the *nos* mutant defect in dendrite morphogenesis. (A–D) Confocal Z-series projections of class IV da neurons in third instar *nos* mutant larvae (A) or *nos* mutant larvae expressing *nos-(ms2)$_{18}$ (B), nos+2-(ms2)$_{18}$ (C),* or *nos+1-(ms2)$_{18}$* (D) transgenes. (E) Quantitation of dendritic terminal branches. Two independent lines for each transgene produced similar results and one line for each is shown. Values are the average +/− standard error for *nos*$^{-}$ (n=11 neurons); *nos-(ms2)$_{18}$* (n=11 neurons); *nos+2-(ms2)$_{18}$* (n=9 neurons); *nos+1-(ms2)$_{18}$* (n=11 neurons).

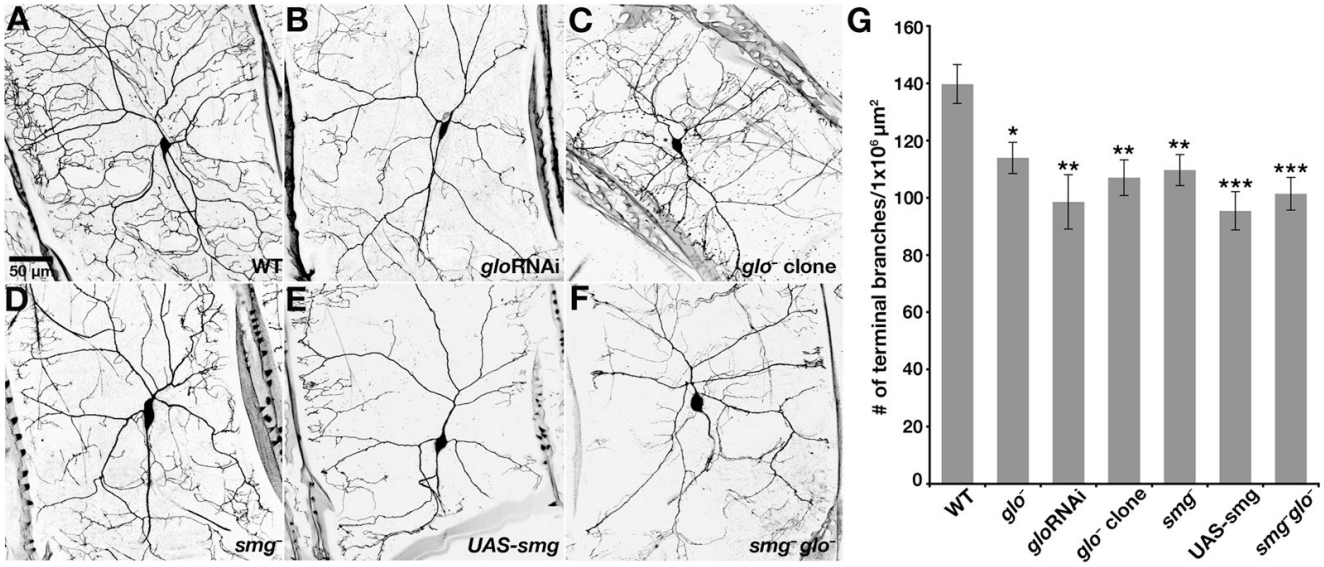

Figure 4. Glo and Smg are Required for Dendrite Development

(A–F) Confocal Z-series projections of class IV da neurons in third instar larvae. (A) Class IV da neuron from a wild-type larva. (B) Neuron from a *glo* RNAi larva. (C) *glo* mutant neuron generated by MARCM. (D) Neuron from a *smg* mutant larva. (E) Neuron from larva overexpressing *smg (UAS-smg*). (F) Neuron from larva doubly mutant for *glo* and *smg*. (G) Quantitation of total number of terminal branches within a 1×10^6 μm^2 region of the dendritic tree of an individual neuron. Values are the average +/− standard error for wild-type (n=15 neurons), *glo*$^-$ (n=10 neurons), *glo*RNAi (n=10 neurons), *glo*$^-$ MARCM clone (n=5 neurons), *smg*$^-$ (n=10 neurons), *UAS-smg* (n=9 neurons) and *smg*$^-$*glo*$^-$ (n=10 neurons).

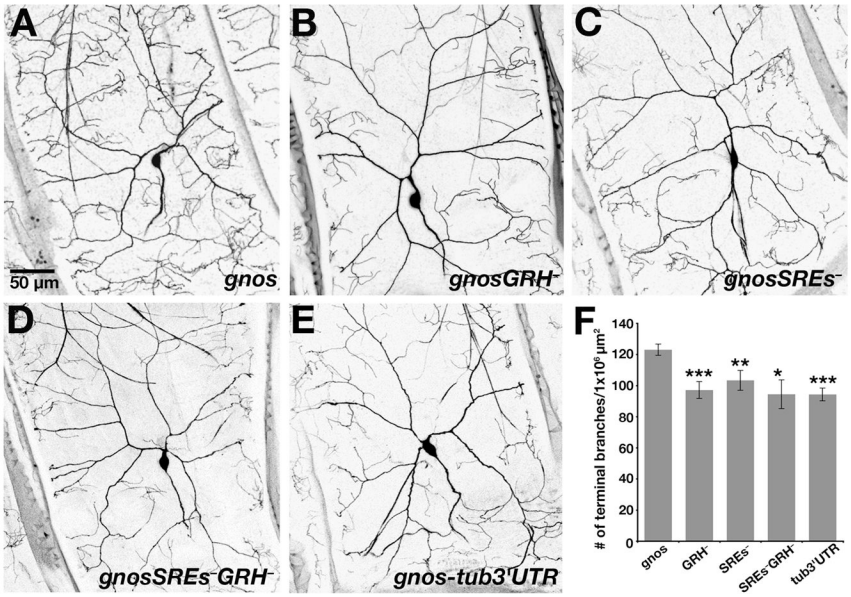

Figure 5. Effect of TCE Mutations on *nos* Regulation in Da Neurons

(A–E) Confocal Z-series projections of class IV da neurons in third instar larvae expressing the (A) *gnos*, (B) *gnosGRH*$^{-}$, (C) *gnosSREs*$^{-}$, (D) *gnosSREs*$^{-}$*GRH*$^{-}$, and (E) *gnos-tub3′UTR* transgenes. (F) Quantitation of dendritic terminal branches. Similar results were obtained from analysis of three independent lines for each transgene and data obtained from one line for each is shown. For each transgene, values are the average +/− standard error: *gnos* (n=9 neurons); *gnosGRH*$^{-}$ (n= 10 neurons); *gnosSREs*$^{-}$ (n=9 neurons); *gnosSREs*$^{-}$*GRH*$^{-}$ (n=8 neurons); *gnos-tub3′UTR* (n=10 neurons).